

Stress Testing Advanced RAIM Airborne Algorithms

Juan Blanch and Todd Walter
Stanford University

ABSTRACT

We describe a methodology to test the integrity of Advanced RAIM algorithms through simulation. To this purpose we describe near worst-case fault magnitudes for multiple simultaneous faults, demonstrate through a set of examples that these faults do indeed achieve close to the worst case integrity risk, and propose an outline of the offline tests to demonstrate the integrity of ARAIM airborne algorithms based on these fault profiles.

INTRODUCTION

GPS L1 based RAIM has been extremely successful. It has provided worldwide horizontal guidance to hundreds of thousands of aircraft since the mid 1990's. However, it does have some limitations. In particular, its performance is quite sensitive to the geometric strength of the GPS constellation. We expect that Advanced RAIM, which will integrate new signals and new constellations, will mitigate these weaknesses, and eventually offer worldwide vertical guidance.

The ARAIM concept was described in [1,2], and further defined in [3,4], and work is ongoing to develop the Standards and Recommended Practices [5] to be included in [6], as well as the receiver standards [7]. The ARAIM reports [1,2] presented several possible architectures, broadcasting options, and a reference airborne algorithm. As part of the concept validation, several prototypes of the airborne algorithm are being evaluated [8-10]. The outline of the proof of safety for the reference algorithm has been established analytically (at least in [11]).

The purpose of this paper is to propose a methodology to demonstrate the safety of advanced RAIM airborne algorithms (including the reference ARAIM algorithm) using simulated faults, and both real and simulated nominal measurements. This methodology could be used as a basis for the offline tests used in the future Minimum Operational Performance Standards for ARAIM to demonstrate compliance with the integrity requirements.

In the first part, we introduce notations and definitions. In the second part, we determine, for each fault mode (even multi-dimensional ones), a set of biases that is representative of the worst case. Based on these faults, in the third part we describe a set of offline tests designed to demonstrate the integrity of fault detection algorithms for ARAIM.

NOTATIONS AND DEFINITIONS

Nominal and fault error model

We use the nominal and fault error model described, among others, in [13] and [14]. In the fault free case, we have:

$$y = Gx + \varepsilon \quad (1)$$

where:

y are the pseudorange measurements,

G is the geometry matrix (n by p)

n is the number of measurements

p the number of states (3 coordinates and $p-3$ clock unknowns)

x is the receiver location and clock offsets (one for each constellation)

ε is the nominal noise and is assumed to be $N(0, W^{-1})$

To start, we consider a very general fault error model:

$$y = Gx + Ab + \varepsilon \quad (2)$$

where:

b is a vector of biases of length m

A is a n by m matrix projecting a set of biases b onto the pseudorange measurements.

Without loss of generality, we assume that the matrix $[G \ A]$ is full rank.

Position estimate and position error

For each state q , we assume an unbiased estimator (which we later restrict to the least squares estimator)

$$\hat{x}_q = e_q^T \hat{x} = s_q^T y \quad (3)$$

where

\hat{x}_q is the estimate of the state

e_q is the vector that selects the q -th state

s_q is the estimator for the q -th state

The position error as a function of the fault bias is given by:

$$\hat{x}_q - x_q = s_q^T \varepsilon + s_q^T Ab \quad (4)$$

The position error distribution is therefore characterized by:

$$\hat{x}_q - x_q \sim N\left(s_q^T A b, s_q^T W^{-1} s_q\right) \quad (5)$$

Test statistics: chi-square

The chi-square statistic [13], [15],[16] is given by:

$$t = y^T P y \quad (6)$$

where:

$$P = W - W G (G^T W G)^{-1} G^T W \quad (7)$$

Under faulted conditions, the test statistics t follows a non-central chi-square with $n-p$ degrees of freedom and non-centrality parameter λ defined by [15]:

$$\lambda = b^T A^T P A b \quad (8)$$

Test statistics: solution separation

The solution separation statistic [11] is composed of the differences between the all-in-view solution and each of the fault tolerant solutions corresponding to each fault mode. Using the notations from [11], the statistic can be written as:

$$t = \max_{q,k} \left\{ \left| \frac{(s_q^{(k)} - s_q) y}{T_{k,q}} \right| \right\} \quad (9)$$

where

$s_q^{(k)}$ is the fault tolerant estimator for fault mode k

$T_{k,q}$ is the corresponding detection threshold (as defined in [11])

Probability of missed detection

The probability of missed detection is the probability that the position error exceeds the region defined by the alert limits or the protection levels (which we will note B_{AL}) and the test statistic remains below a pre-defined threshold T . For a given set of biases (as in Equation (2)), this probability is given by:

$$P_{md}(b) = P(\hat{x} - x \notin B_{AL}, t \leq T | b) \quad (10)$$

As mentioned above, the fault detection algorithm must protect against any b , so the integrity risk given a fault is given by:

$$\bar{P}_{md} = \max_b P_{md}(b) \quad (11)$$

The goal of the next section is to determine the b that realizes the maximum (or at least gets close to it) that is:

$$\bar{P}_{md} = P_{md}(b_{\max}) \quad (12)$$

NEAR WORST-CASE FAULT FOR EACH FAULT MODE

In this section, we determine near worst-case fault magnitudes for a given fault mode. Fault modes in ARAIM are defined as sets of measurements that have arbitrary biases. ARAIM must protect the user against the worst-case bias. A worst case fault is one that maximizes the integrity risk. However, the integrity risk is dependent on the test statistic and the threshold used by the algorithm. As a consequence, given a fault mode, the worst-case fault is dependent on the test statistic. We show that for two of well-known test statistics used in ARAIM the worst case profile is not very dependent on the test statistic.

Here we derive the following:

1. The exact worst-case fault for the chi-square statistic for one coordinate
2. An approximate worst-case fault for the horizontal error for the chi-square statistic
3. An approximate worst-case fault for the solution separation for one coordinate
4. An approximate worst-case fault for the horizontal error for the solution separation statistic

For all these, we will assume that the all-in-view solution is computed using a least square estimate, that is:

$$s_q^T = e_q^T (G^T W G)^{-1} G^T W \quad (13)$$

With this estimator, the position error and the measurement residuals are uncorrelated, and therefore independent, and since the test statistic is a function of the measurement residuals, the position error and the test statistic are independent. We can write:

$$P_{md}(b) = P(\hat{x} - x \notin B_{AL} | b) P(t \leq T | b) \quad (14)$$

Case of chi-square statistic and one coordinate

For this case we can replace the terms in Equation (14) with more explicit expressions:

$$P(\hat{x} - x \notin B_{AL} | b) = P(|s_q^T \varepsilon + s_q^T Ab| > L) = Q\left(\frac{L - s_q^T Ab}{\sigma_q}\right) + Q\left(\frac{L + s_q^T Ab}{\sigma_q}\right) \quad (15)$$

$$P(t \leq T | b) = P_{ncx}(T, n-p, \lambda) \quad (16)$$

where

$P_{ncx}(T, n-p, \lambda)$ is the non-central cdf evaluated at T , with $n-p$ degrees of freedom, and non-centrality parameter λ (defined in Equation (8)).

Q is the tail cdf of a normal distribution

$$\sigma_q = \left[(G^T W G)^{-1} \right]_{q,q}$$

The probability of missed detection is then given by:

$$P_{md}(b) = \left(Q\left(\frac{L - s_q^T Ab}{\sigma_q}\right) + Q\left(\frac{L + s_q^T Ab}{\sigma_q}\right) \right) P_{ncx}(T, n-p, b^T A^T P A b) \quad (17)$$

The upper bound if this expression can be computed in two steps. Here we provide a variant of the methods proposed in [15],[16].

For a fixed non-centrality parameter λ , the P_{md} will be maximized with the largest possible position error bias. That is, we solve (we drop the index q to lighten the notations):

$$\begin{aligned} & \max |s^T Ab| \\ & \text{Subject to } b^T A^T P A b = \lambda \end{aligned} \quad (18)$$

There are many ways of solving the above optimization. One way is by writing:

$$|s^T Ab| = \left| s^T A (A^T P A)^{-\frac{1}{2}} (A^T P A)^{\frac{1}{2}} b \right| \quad (19)$$

Applying the Cauchy-Schwarz inequality, we get:

$$\begin{aligned} |s^T Ab|^2 &= \left| s^T A (A^T P A)^{-\frac{1}{2}} (A^T P A)^{\frac{1}{2}} b \right|^2 \leq \left(s^T A (A^T P A)^{-1} A^T s \right) (b^T A^T P A b) \\ &\leq \left(s^T A (A^T P A)^{-1} A^T s \right) \lambda \end{aligned} \quad (20)$$

Equality is achieved when:

$$\left(A^T PA\right)^{\frac{1}{2}} b \propto \left(A^T PA\right)^{-\frac{1}{2}} A^T s \text{ or equivalently: } b = \alpha \left(A^T PA\right)^{-1} A^T s \quad (21)$$

where α is a scalar factor.

The solution of the problem defined by (18) is therefore:

$$\max |s^T Ab| = \sqrt{\lambda} \sqrt{s^T A \left(A^T PA\right)^{-1} A^T s} \quad (22)$$

We have:

$$\sqrt{s^T A \left(A^T PA\right)^{-1} A^T s} = \sigma_{ss,q}^{(A)} = \sqrt{\sigma_q^{(A)2} - \sigma_q^{(0)2}} \quad (23)$$

where $\sigma_q^{(0)}$, $\sigma_q^{(A)}$, and $\sigma_{ss,q}^{(A)}$ are respectively the standard deviations of the all-in-view solution, of the fault tolerant solution, and of the solution separation. This is shown in [16], [17] and a proof is given in Appendix A.

The maximum is attained at:

$$b = \frac{\sqrt{\lambda}}{\sigma_{ss,q}^{(A)}} \left(A^T PA\right)^{-1} A^T s \quad (24)$$

The problem is now reduced to finding the worst case non-centrality parameter. This can be now solved numerically by maximizing:

$$P_{md}(b) = \left(Q \left(\frac{L - \sqrt{\lambda} \sigma_{ss,q}^{(A)}}{\sigma_q} \right) + Q \left(\frac{L + \sqrt{\lambda} \sigma_{ss,q}^{(A)}}{\sigma_q} \right) \right) P_{ncx}(T, n - p, \lambda) \quad (25)$$

Particular case: subset solution

We examine the case of a subset solution, and provide a more practical expression for (24). In the Appendix, we show that we have:

$$\left(A^T PA\right)^{-1} A^T s_q = \tilde{G} \left(\tilde{G}^T \bar{W} \bar{G}\right)^{-1} e_q \quad (26)$$

where:

\tilde{G} corresponds to the lines of sight in the observation matrix that are faulted

\bar{G} corresponds to the remaining lines of sight

In the Appendix, we also show that the formula is valid in the case of a constellation wide fault, as long as we replace the above matrices with ones where the coordinate corresponding to the

clock of the faulted constellation has been removed. This formula shows that the worst case fault has the effect of a position solution offset on the faulted measurements. This position offset is derived from the covariance of the fault free measurements.

Approximate worst-case fault for the horizontal error for the chi-square statistic

In this case, we have:

$$P(\hat{x} - x \notin B_{AL} | b) = P\left(\left|s_1^T \varepsilon + s_1^T Ab\right|^2 + \left|s_2^T \varepsilon + s_2^T Ab\right|^2 > L^2\right) \quad (27)$$

The expression is difficult to maximize. It is tempting (and possible) to simply maximize the norm of the vector β defined by:

$$\beta = \begin{bmatrix} s_1^T Ab \\ s_2^T Ab \end{bmatrix} \quad (28)$$

This approach does ignore the effect of the distribution of the nominal error, so we will attempt a slightly different approach. Let us first consider a vector of biases b_{max} that maximizes the expression (27) above. We consider the rotation in the horizontal plane that aligns the first coordinate with the vector β_{max} (defined by Equation (28)). We have:

$$\left|s_1^T \varepsilon + s_1^T Ab\right|^2 + \left|s_2^T \varepsilon + s_2^T Ab\right|^2 = \left|s_1^T(\theta) \varepsilon + s_1^T(\theta) Ab\right|^2 + \left|s_2^T(\theta) \varepsilon\right|^2 \quad (29)$$

where ϑ is the rotation angle and:

$$s_1(\theta) = \cos(\theta) s_1 + \sin(\theta) s_2$$

$$s_2(\theta) = -\sin(\theta) s_1 + \cos(\theta) s_2$$

We now make the approximation (which does not need to be an upper bound, since we are only looking for the argument of the maximum) that:

$$P\left(\left|s_1^T(\theta) \varepsilon + s_1^T(\theta) Ab\right|^2 + \left|s_2^T(\theta) \varepsilon\right|^2 > L^2\right) \sim P\left(\left|s_1^T(\theta) \varepsilon + s_1^T(\theta) Ab\right|^2 > L^2\right) \quad (30)$$

With this approximation, we can use the result corresponding to the one coordinate case (Equation (24)). For a given angle θ , the worst case direction is approximated by:

$$b(\theta) = \frac{\sqrt{\lambda}}{\sigma_{ss,q}^{(A)}(\theta)} (A^T P A)^{-1} A^T s_1(\theta) \quad (31)$$

Where $\sigma_{ss,q}^{(A)}(\theta)$ is the solution separation statistic projected along the direction defined by θ .

For subset faults, using Equation (26), we get:

$$b(\theta) = \frac{\sqrt{\lambda}}{\sigma_{ss,q}^{(A)}(\theta)} \tilde{G} (\bar{G}^T \bar{W} \bar{G})^{-1} e(\theta) \quad (32)$$

where

$$e(\theta) = [\cos(\theta) \quad \sin(\theta) \quad 0 \quad \dots \quad 0]^T$$

To find an approximate worst case magnitude for a given θ , we need to solve the numerical problem (where λ is the unknown):

$$\max_{\lambda} \left(Q \left(\frac{L - \sqrt{\lambda} \sigma_{ss,q}^{(A)}(\theta)}{\sigma_q(\theta)} \right) + Q \left(\frac{L + \sqrt{\lambda} \sigma_{ss,q}^{(A)}(\theta)}{\sigma_q(\theta)} \right) \right) P_{ncx}(T, n-p, \lambda) \quad (33)$$

Ideally, we would like to solve this problem for all values of θ and take the maximum. In practice, we will choose a discretization of the interval $[0 \pi]$.

Approximate worst case for the solution separation statistic for one coordinate

For the solution separation statistic, the function we need to maximize is given by:

$$P_{md}(b) = \left(Q \left(\frac{L - s_q^T Ab}{\sigma_q} \right) + Q \left(\frac{L + s_q^T Ab}{\sigma_q} \right) \right) P \left(\max_{q',k} \left\{ \left| \frac{(s_{q'}^{(k)} - s_{q'}) \varepsilon + (s_{q'}^{(k)} - s_{q'}) Ab}{T_{k,q'}} \right| \leq 1 \right\} \right) \quad (34)$$

An exact solution to this problem would in general be very computationally costly, because it involves the integration of a multivariate gaussian over a simplex.

Instead we will make the assumption that minimizing the right side term of the product is approximately equivalent to minimizing the sum of squares of the magnitude of the biases in each statistic. In order to keep the same structure as before, we will consider the dual problem (maximizing the position solution bias). That is, we solve:

$$\begin{aligned} & \max_b |s_q^T Ab| \\ & \text{s.t.} \quad \sum_{q',k} \left| (s_{q'}^{(k)} - s_{q'}) Ab \right|^2 = \lambda \end{aligned} \quad (35)$$

We can rewrite this problem as follows:

$$\begin{aligned} & \max_b |s_q^T Ab| \\ & \text{s.t.} \quad b^T A^T Q Ab = \lambda \end{aligned} \quad (36)$$

where

$$Q = \sum_{q',k} \left(s_{q'}^{(k)} - s_{q'} \right)^T \left(s_{q'}^{(k)} - s_{q'} \right) \quad (37)$$

We now notice that the problem (36) is formally identical to (18). Therefore, the solution is of the form:

$$b = \alpha \left(A^T Q A \right)^{-1} A^T s_q \quad (38)$$

Like before, we need to find the scale factor α that maximizes the P_{md} . For this step, we make the approximation:

$$P \left(\max_{q',k} \left\{ \left| \frac{\left(s_{q'}^{(k)} - s_{q'} \right) \mathcal{E} + \left(s_{q'}^{(k)} - s_{q'} \right) A b}{T_{k,q'}} \right| \leq 1 \right\} \right) \sim P \left(\left| \frac{\left(s_q^{(k_A)} - s_q \right) \mathcal{E} - s_q^T A b}{\sigma_{ss,q}^{(A)}} \right| \leq \frac{T_{k_A,q}}{\sigma_{ss,q}^{(A)}} \right) \quad (39)$$

The problem consists then in maximizing the one-dimensional function:

$$P_{md}(b) = \left(Q \left(\frac{L-z}{\sigma_q} \right) + Q \left(\frac{L+z}{\sigma_q} \right) \right) \left(Q \left(\frac{z - T_{k_A,q}}{\sigma_{ss,q}^{(A)}} \right) - Q \left(\frac{z + T_{k_A,q}}{\sigma_{ss,q}^{(A)}} \right) \right) \quad (40)$$

where $z = s_q^T A b$. As before, this is done numerically. Once we find the argument realizing the maximum z_{max} , we determine the scale factor α with the equation:

$$z_{max} = s_q^T A b \quad (41)$$

Approximate worst-case fault for the horizontal error for the solution separation statistic

Using approximations and a method similar to the ones used in the second case (chi-square statistic and horizontal error), we determine an approximate worst-case fault as follows. For each value of θ we determine $z_{max}(\theta)$ using Equation (40) for the coordinate rotated by θ . We then choose the value of $\theta = \theta_{max}$ that maximizes the P_{md} , and define the vector b_{max} as:

$$b_{max} = \frac{z_{max}}{s_1^T(\theta) A \left(A^T Q A \right)^{-1} A^T s_1(\theta)} \left(A^T Q A \right)^{-1} A^T s_1(\theta) \quad (42)$$

Summary

We note that, in fact, Q and P have similar properties: they are both weighted projections whose kernel is defined by the matrix G. For this reason, we expect the near worst case faults

defined above for both test statistics to be quite similar. In the next section, the faults will be determined by:

$$b_{\max} = \frac{z_{\max}}{\sigma_{ss,q}^{(A)}(\theta)} \tilde{G}(\bar{G}^T \bar{W} \bar{G})^{-1} e(\theta) \quad (43)$$

with z_{\max} defined by Equation (40).

EVALUATION OF NEAR WORST-CASE FAULTS: EXAMPLES

For the two detection statistics considered above, upper bounds on the P_{md} can be determined using Equations (25) and Equation (40). In the case of one coordinate and the chi-square statistic, we know that the worst case determined above realizes the computed P_{md} . For the other cases, we show through examples that these faults get quite close to the computed upper bound.

We examine the case of one coordinate and the solution separation statistic. We consider the geometry described in Appendix B. For this example we chose:

- An Alert limit of 50 m
- A P_{fa} of 4×10^{-6}

For a given fault mode, the direction of the simulated fault was defined by Equation (32), and its modulus was defined by Equation (41). The resulting vector is given in Appendix B. We simulated 10000 samples of nominal measurements (following the statistics defined by the nominal noise) and ran the detection tests on them.

Example 1: Fault mode corresponding to the constellation wide failure of Galileo

The algorithm tested all the one out solution separation statistics as well as the Galileo out one. For the constellation wide fault of Galileo, the upper bound on the P_{md} computed using Equation (40) was 3.5×10^{-2} . In the simulation, there were 362 integrity failures (cases where the error exceeded the Alert Limit and the tests did not trip). The empirical P_{md} was therefore 3.62×10^{-2} , which, compared to the theoretical upper bound of 3.5×10^{-2} , shows that the simulated faulted achieves the worst case P_{md} .

Example 2: Fault mode corresponding to one out GPS and one out Galileo

For this example, we looked at a scenario where the simultaneous fault of two satellites must be monitored. We considered the failure mode corresponding to the 5th GPS satellite and the 3rd Galileo satellite from the geometry described in Appendix B. The upper bound on the P_{md} using Equation (40) was 0.78. In the simulation, we found that the fault defined as described above resulted in 7700 integrity failures. This corresponds to a 0.77 empirical P_{md} , which is very close to the upper bound of 0.78.

We note that this is not a trivial result. To demonstrate this, let us consider the same fault mode, but where we have changed the magnitude in the Galileo satellite to -80. In this case, the

empirical P_{md} is 0: the fault was always detected in time. Figure 1 shows the empirical P_{md} as a function of the fault magnitude in the Galileo satellite for a range of values (for the figures, we only simulated 1000 samples).

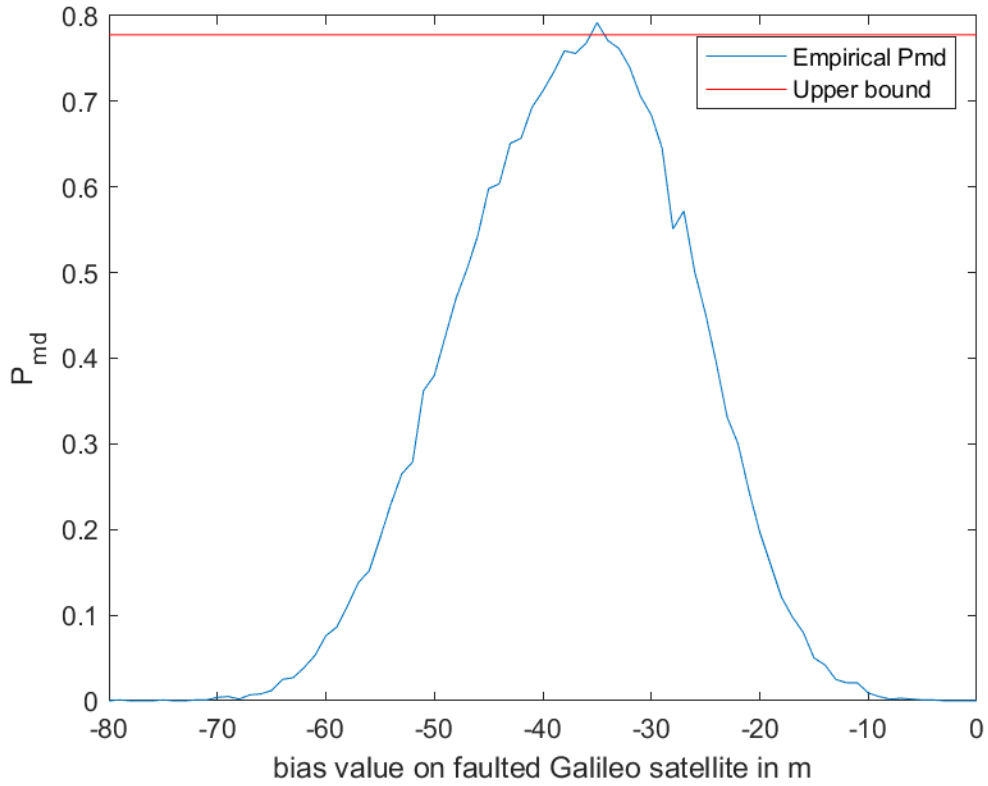


Figure 1. Empirical P_{md} as a function of the bias in second faulted satellite (while fault is fixed in first satellite)

Figure 2 shows the empirical P_{md} also as a function of the Galileo fault magnitude, but where we have forced the projection of the error to remain at its worst case value.

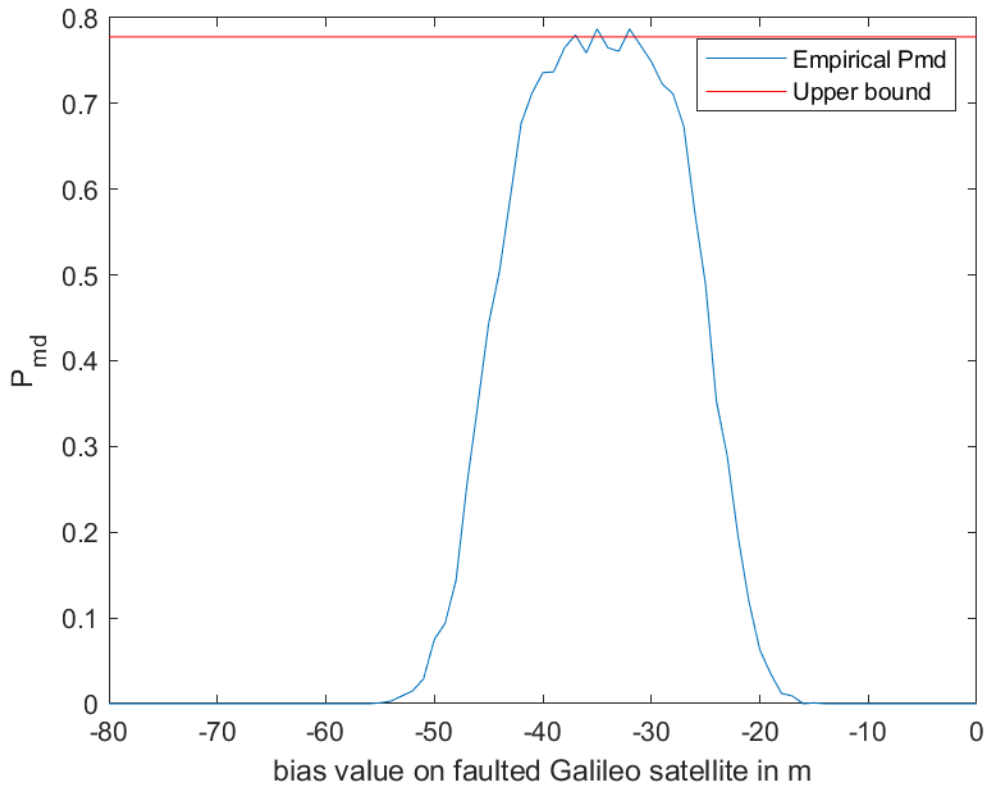


Figure 2. Empirical P_{md} as a function of the bias in second faulted satellite (while fault bias in first satellite is adjusted to maintain a fixed bias in the position domain)

These two examples strongly suggest that, first, the candidate worst-case faults defined in the previous section get very close to realizing the worst case fault, and second, that the choice of the fault magnitude is critical to adequately test the fault detection algorithm. In Figure 3, we test the subset faults for which the expected contribution exceeds 10^{-3} . Again, we can see that the simulated faults achieve close to the worst case upper bound in every case.

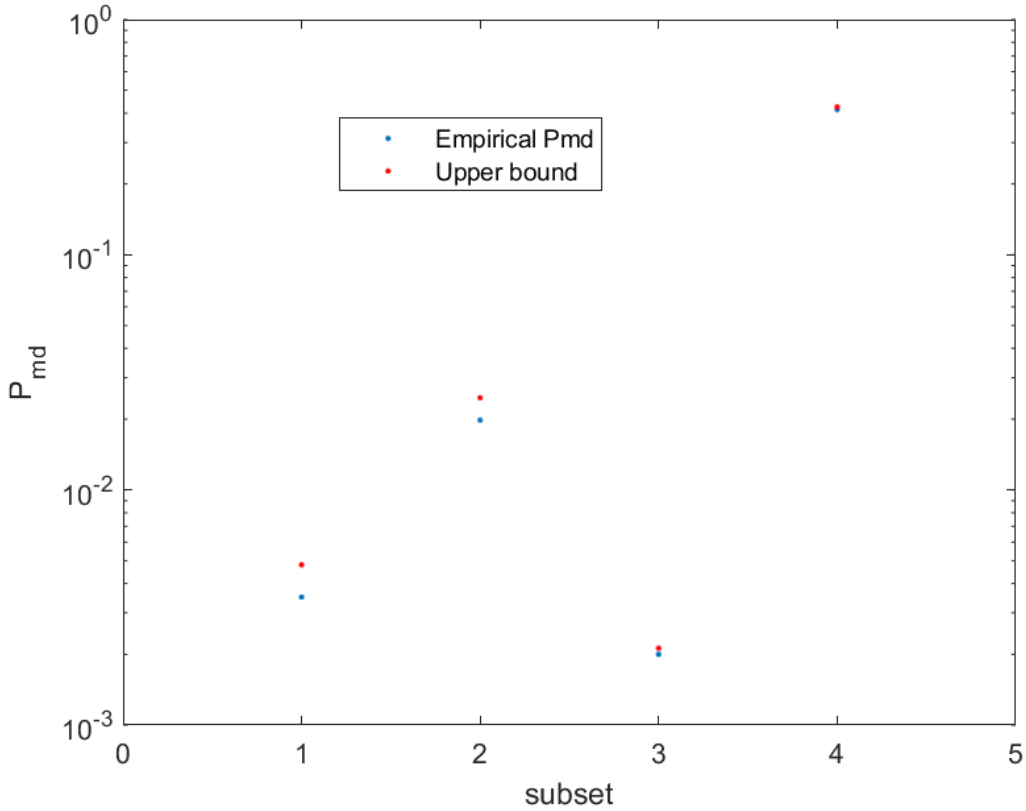


Figure 3. Empirical P_{md} and upper bound for the subset faults with the largest contribution in the example geometry

DEMONSTRATION OF INTEGRITY REQUIREMENTS THROUGH NUMERICAL TESTS

Based on the worst case faults determined in the previous section, here we propose an approach to design the set of offline tests similar to the ones used to ensure that the integrity of RAIM FDE algorithms in [8]. In ARAIM, the fixed probability of missed detection requirement in RAIM is replaced by a more general integrity requirement in ARAIM, so the tests must be modified to account for this difference. To address this point, we use an approach similar to the one presented in [12], which consists in defining a generalized probability of missed detection.

The tests must show empirically that the integrity risk is met. That is, we need to have:

$$P(HMI) = P\left(\left(\hat{x}(t) - x(t) \notin B_{AL} \text{ \& no alert within 10 s}\right) \text{ for } t \text{ over 1 h}\right) \leq 10^{-7} \quad (44)$$

The integrity parameters allow the user to compute all the fault hypotheses H_k . In this first proposal, we will assume that the fault is either present throughout the whole exposure window or not present. This assumption, which greatly simplifies the design of the tests, may be revisited in the future. We re-write Equation (44) using the formula of total probability:

$$P(HMI) = P(HMI | H_0)P(H_0) + \sum_{k \geq 1} P(HMI | H_k)P(H_k) \quad (45)$$

Based on this equation, it would be possible to design the tests by creating a set of measurement N_{sample} samples as follows:

- 1) Determine randomly which fault mode will be active. This would be done according to the probabilities $P(H_k)$.
- 2) Determine the fault magnitude for H_k as described above
- 3) Generate N_{exp} nominal error samples per satellite to represent the measurements over the whole exposure window (N_{exp} of 360 may be sufficient)
- 4) Determine whether this set of measurements combined with the fault lead to an HMI event

This process would be repeated for a sufficient number of samples. The empirical integrity risk would be the number of HMI events over the total number of samples N_{sample} .

The issue with this approach is that the number of necessary samples would be very high: to reach probabilities of 10^{-7} , we may have to simulate 10^8 samples or more (and this would be for one geometry only). As suggested in [12], we can drastically reduce the number required samples by noticing that the first term in (45) can be computed analytically with simple assumptions (in practice this term is usually negligible). We therefore only need to demonstrate that:

$$\sum_{k \geq 1} P(HMI | H_k)P(H_k) \leq 10^{-7} - P(HMI | H_0)P(H_0) \quad (46)$$

The above inequality is equivalent to:

$$\sum_{k \geq 1} P(HMI | H_k) \frac{P(H_k)}{\sum_{k \geq 1} P(H_k)} \leq \frac{10^{-7} - P(HMI | H_0)P(H_0)}{\sum_{k \geq 1} P(H_k)} \quad (47)$$

The denominator is the probability that there is a fault during the exposure window. This probability, while dynamic, is expected to be below 10^{-3} in the worst case. As a consequence, the right hand side term will be on the order of 10^{-4} , which now results in a more feasible number of samples. The above method is therefore modified as follows. For each sample:

- 1) Determine randomly which fault mode will be active. This would be done according to the probabilities $\tilde{P}(H_i)$, where:

$$\tilde{P}(H_i) = \frac{P(H_i)}{\sum_{k \geq 1} P(H_k)} \quad (48)$$

- 2) Determine the fault magnitude for H_i as described above
- 3) Generate N_{exp} nominal error samples per satellite to represent the measurements over the whole exposure window (N_{exp} of 360 may be sufficient)
- 4) Determine whether this set of measurements combined with the fault lead to an HMI event

The main difference with the previous method is the number of samples, which now is only

required to be on the order of $\frac{\sum_{k \geq 1} P(H_k)}{10^{-7} - P(HMI | H_0)P(H_0)}$.

In addition, the tests will need to specify:

- The values of the integrity parameters (Rsat, Rconst, MTTN)
- The user geometries
- The nominal error parameters (including the parameters determining the temporal decorrelation of the errors)

The final version of this paper will include the results of these tests applied to the reference ARAIM airborne algorithm ([1],[11], both with simulated data and real data.

SUMMARY

We have described a methodology to test the integrity of Advanced RAIM algorithms through simulation. To this purpose, we have developed a simple formula for near worst-case fault magnitudes for multiple simultaneous faults, and demonstrated through a set of examples that these faults do indeed achieve close to the worst case integrity risk. Finally, we have propose an outline of the offline tests to demonstrate the integrity of ARAIM airborne algorithms based on these fault profiles.

REFERENCES

- [1] Working Group C, ARAIM Technical Subgroup, Milestone 3 Report, February 26, 2016. Available at:
<http://www.gps.gov/policy/cooperation/europe/2016/working-group-c/>
http://ec.europa.eu/growth/tools-databases/newsroom/cf/itemdetail.cfm?item_id=8690
- [2] Working Group C, ARAIM Technical Subgroup, Milestone 2 Report, Issue 1.0, February 11, 2015. Available at:
<http://www.gps.gov/policy/cooperation/europe/2015/working-group-c/>
http://ec.europa.eu/growth/tools-databases/newsroom/cf/itemdetail.cfm?item_id=8191
- [3] Blanch, Juan, Walter, Todd, Enge, Per, Burns, Jason, Mabillean, Mikael, Martini, Ilaria, Boyero, Juan Pablo, Berz, Gerhard, "A Proposed Concept of Operations for Advanced Receiver Autonomous Integrity Monitoring," *Proceedings of the 31st International Technical Meeting of The Satellite Division of the Institute of Navigation (ION GNSS+ 2018)*, Miami, Florida, September 2018, pp. 1084-1090.
- [4] ARAIM CONOPS, posted in ICAO NSP as JWG/3 WP38 available upon demand
- [5] Draft of ARAIM SARPS, ICAO NSP Working Paper, posted as JWG/4 IP32
- [6] ICAO, Annex 10, Aeronautical Telecommunications, Volume 1 (Radio Navigation Aids), Seventh Edition including Amendment 91, published July 2018, effective 8 November 2018.
- [7] Blanch et al. "Development of the ARAIM MOPS" *Proceedings of the 32nd International Technical Meeting of The Satellite Division of the Institute of Navigation (ION GNSS+ 2019)*, Miami, Florida, September 2019
- [8] Phelts, R. Eric, Blanch, Juan, Gunning, Kazuma, Walter, Todd, Enge, Per, "Assessing of Aircraft Banking on ARAIM Performance," *Proceedings of the 31st International Technical Meeting of*

The Satellite Division of the Institute of Navigation (ION GNSS+ 2018), Miami, Florida, September 2018, pp. 2632-2641.

[9] Phelts, R. Eric, Blanch, Juan, Chen, Yu-Hsuan, Enge, Per, Riley, Stuart, "ARAIM in Flight Using GPS and GLONASS: Initial Results from a Real-time Implementation," *Proceedings of the 29th International Technical Meeting of The Satellite Division of the Institute of Navigation (ION GNSS+ 2016)*, Portland, Oregon, September 2016, pp. 3264-3269.

[10] Blanch, Juan, Phelts, R. Eric, Chen, Yu-Hsuan, Enge, Per, "Initial Results of a Multi-Constellation ARAIM Airborne Prototype," *Proceedings of the 2017 International Technical Meeting of The Institute of Navigation*, Monterey, California, January 2017, pp. 184-209.

[11] Blanch, J., Walter, T., Enge, P., Lee, Y., Pervan, B., Rippl, M., Spletter, A., Kropp, V., "Baseline Advanced RAIM User Algorithm and Possible Improvements," *IEEE Transactions on Aerospace and Electronic Systems*, Volume 51, No. 1, January 2015.

[12] Bouvet, Denis. "Offline test procedures for ARAIM", briefing presented in EUROCAE WG-62, September 2019.

[13] Blanch, J., Walter, T., and Enge, P., "Optimal Positioning for Advanced RAIM," *NAVIGATION*, Vol. 60, No. 4, Winter 2013, pp. 279-290.

[14] Blanch, Juan, Walter, Todd, Enge, Per, "Theoretical Results on the Optimal Detection Statistics for Autonomous Integrity Monitoring", *NAVIGATION, Journal of The Institute of Navigation*, Vol. 64, No. 1, Spring 2017, pp. 123-137.

[15] Angus, J. E., "RAIM with Multiple Faults", *NAVIGATION, Journal of The Institute of Navigation*, Vol. 53, No. 4, Winter 2006-2007, pp. 249-257.

[16] Joerger, M., Chan, F.-C., Pervan, B., "Solution Separation Versus Residual-Based RAIM", *NAVIGATION, Journal of The Institute of Navigation*, Vol. 61, No. 4, Winter 2014, pp. 273-291.

[17] Blanch, J., Walter, T., Enge, P. "RAIM with Optimal Integrity and Continuity Allocations Under Multiple failures," *IEEE Transactions on Aerospace and Electronic Systems* Vol. 46, No. 3, July 2010.

APPENDIX A

Relationship between slope and solution separation

By definition, we have:

$$s^T A (A^T P A)^{-1} A^T s = e^T (G^T W G)^{-1} G^T W A (A^T W A - A^T W G (G^T W G)^{-1} G^T W A)^{-1} A^T W G (G^T W G)^{-1} e \quad (49)$$

The covariance of the fault tolerant subset solution Cov_A is given by (using the matrix inversion lemma):

$$\text{Cov}_A = \begin{bmatrix} G^T W G & G^T W A \\ A^T W G & A^T W A \end{bmatrix}^{-1} = \begin{bmatrix} (G^T W G)^{-1} + (G^T W G)^{-1} G^T W A Z^{-1} A^T W G (G^T W G)^{-1} & -(G^T W G)^{-1} G^T W A Z^{-1} \\ -Z^{-1} A^T W G (G^T W G)^{-1} & Z^{-1} \end{bmatrix} \quad (50)$$

where:

$$Z = A^T W A - A^T W G (G^T W G)^{-1} G^T W A \quad (51)$$

We therefore have:

$$\begin{aligned} \sigma_q^{(A)2} &= e_q^T (G^T W G)^{-1} e_q + e_q^T (G^T W G)^{-1} G^T W A Z^{-1} A^T W G (G^T W G)^{-1} e_q \\ &= \sigma_q^2 + s^T A (A^T P A)^{-1} A^T s \end{aligned} \quad (52)$$

As a consequence:

$$s^T A (A^T P A)^{-1} A^T s = \sigma_q^{(A)2} - \sigma_q^{(0)2} = \sigma_{ss,q}^{(A)} \quad (53)$$

The last equality is shown in [16], and is a direct consequence of the fact that:

$$S W^{-1} (S - S_A)^T = (G^T W G)^{-1} G^T (S - S_A)^T = (G^T W G)^{-1} (I - I) = 0 \quad (54)$$

where:

$$S = (G^T W G)^{-1} G^T W$$

and S_A can be any unbiased estimator.

Proof of Equation (26)

This equation is given directly by considering the two forms of the matrix inversion lemma (one of the forms being the one given in Equation (50)). Writing the two off-diagonal terms, we get:

$$\begin{aligned} Z^{-1} A^T W G (G^T W G)^{-1} &= (A^T W A)^{-1} A^T W G \left(G^T W G - G^T W A (A^T W A)^{-1} A^T W G \right)^{-1} \\ &= \tilde{G} (\tilde{G}^T \tilde{W} \tilde{G})^{-1} \end{aligned} \quad (55)$$

We now examine how to extend this formula to the case where $(\tilde{G}^T \tilde{W} \tilde{G})^{-1}$ is not invertible due to the clock offset of the faulted constellation.

Due to the clock offset, neither the position solution nor the resulting residuals are changed by a common bias in all the measurements from one constellation. In particular, we can assume that one of them is fault free. We consider the covariance of the fault free measurements by

separating the line of sight from the faulted constellation that we assume to be fault free, we have:

$$(\bar{G}^T \bar{W} \bar{G})^{-1} = \begin{bmatrix} \bar{G}_r^T \bar{W}_r \bar{G}_r + g w g^T & g w \\ g^T w & w \end{bmatrix}^{-1} = \begin{bmatrix} (\bar{G}_r^T \bar{W}_r \bar{G}_r)^{-1} & (\bar{G}_r^T \bar{W}_r \bar{G}_r)^{-1} g w \\ -w g^T (\bar{G}_r^T \bar{W}_r \bar{G}_r)^{-1} & g^T (\bar{G}_r^T \bar{W}_r \bar{G}_r)^{-1} g \end{bmatrix} \quad (56)$$

where $\bar{G} = \begin{bmatrix} \bar{G}_r & 0 \\ g^T & 1 \end{bmatrix}$, and the subscript r means that we have removed the column of 0s corresponding to the faulted constellation. We have:

$$\begin{aligned} \tilde{G} (\bar{G}^T \bar{W} \bar{G})^{-1} e &= \begin{bmatrix} \tilde{G}_r & \underline{1} \end{bmatrix} \begin{bmatrix} (\bar{G}_r^T \bar{W}_r \bar{G}_r)^{-1} & (\bar{G}_r^T \bar{W}_r \bar{G}_r)^{-1} g \\ -g^T (\bar{G}_r^T \bar{W}_r \bar{G}_r)^{-1} & g^T (\bar{G}_r^T \bar{W}_r \bar{G}_r)^{-1} g \end{bmatrix} \begin{bmatrix} e_r \\ 0 \end{bmatrix} = \\ &= \begin{bmatrix} \tilde{G}_r & \underline{1} \end{bmatrix} \begin{bmatrix} (\bar{G}_r^T \bar{W}_r \bar{G}_r)^{-1} e_r \\ -g^T (\bar{G}_r^T \bar{W}_r \bar{G}_r)^{-1} e_r \end{bmatrix} = \tilde{G}_r (\bar{G}_r^T \bar{W}_r \bar{G}_r)^{-1} e_r - g^T (\bar{G}_r^T \bar{W}_r \bar{G}_r)^{-1} e_r \underline{1} \end{aligned} \quad (57)$$

Now let us assume that we add the bias $g^T (\bar{G}_r^T \bar{W}_r \bar{G}_r)^{-1} e_r$ to all the measurements in the faulted constellation. As mentioned above, this does not affect the residuals or the position solution. The faulted biases can be expressed as:

$$b = \alpha \begin{bmatrix} \tilde{G}_r \\ g^T \end{bmatrix} (\bar{G}_r^T \bar{W}_r \bar{G}_r)^{-1} e_r \quad (58)$$

APPENDIX B

The user geometry assumed in the examples is given by:

```
G = [0.0225  0.9951 -0.0966  1 0.0000;
      0.6750 -0.6900 -0.2612  1 0.0000;
      0.0723 -0.6601 -0.7477  1 0.0000;
      -0.6379 -0.2431 -0.7308  1 0.0000;
      -0.9398  0.2553 -0.2269  1 0.0000;
      -0.6748  0.4356 -0.5957  0 1.0000;
      0.0938 -0.7004 -0.7075  0 1.0000;
      0.5571  0.3088 -0.7709  0 1.0000;
      0.9767  0.0298 -0.2125  0 1.0000;
      0.6622  0.6958 -0.2780  0 1.0000];
```

The measurement noise is set at 4 m for all measurements.

The near worst-case fault for the constellation wide fault for the example is given by:

$b = [0 \quad 0 \quad 0 \quad 0 \quad 0 \quad -50.5 \quad -40.5 \quad -82.3 \quad -35.0 \quad -54.1];$

For the dual fault, the worst case fault was given by:

$b = [0 \quad 0 \quad 0 \quad 0 \quad 33.0 \quad 0 \quad 0 \quad -35.5 \quad 0 \quad 0];$